Design of Multi-Mode Low-Frequency Vibration Suppressor Based on Dynamic Vibration Absorption Principle

Yipeng Cheng, Zilong Peng and Huabing Wen

School of Energy and Power, Jiangsu University of Science and Technology, Zhenjiang 212100, China.
E-mail: zlp_just@sina.com

Hao Song and Zixian Cui

Systems Engineering Research Institute, Beijing 100036, China.

(Received 17 February 2022; accepted 15 June 2022)

Dynamic vibration absorbers (DVA) are commonly studied for their advantage in controlling the low-frequency resonance peaks, but most relevant studies are still at the stage of theoretical innovation such as nonlinearity parameters and active control. Nevertheless, there are few kinds of vibration suppression structures based on dynamic vibration absorption principle. In this paper, therefore, we proposed a novel vibration suppressor inspired by the DVA theory. The vibration of a four-sided simply-supported thin plate attached with the DVAs array was studied by applying the modal superposition method. A preliminary suppressor model was proposed with rubber and steel as its main material, and whose modal frequency is calculated theoretically. Geometric and material parameters of each component were adjusted based on the DVA parameters. The vibration control effect of the suppressors array was verified through simulation and by experiment. Results showed that three resonance peaks were suppressed, and it was obvious after the attachment to the DVAs array or suppressors array. The contact form between the suppressors array and the plate is surface contact, which is different from the point contact between the DVAs array and the plate, therefore the vibration control effect of vibration suppressors array is more obvious.

1. INTRODUCTION

The vibration of an engine and pipeline, which may cause discomfort among crews and damage to equipment, is transmitted to the ship's hull and the cabin during ship operation. The acoustic radiation caused by such vibration will weaken stealth performance and the combat ability of naval vessels, especially in submarines. The vibration mentioned above is mainly in the low-frequency domain, which is difficult to control practically. This receives much concern from researchers. Dynamic vibration absorbers (DVAs) are widely used in vibration[1,2] and noise control[3,4] since they have simple configurations and can effectively control the vibration of mechanical systems when properly designed. The concept of the DVA was first proposed by Frahm.[5] After nearly a century's development, the application of nonlinear[6–8] and active control[9–11] has recently become a major field of research of the DVA due to their excellent behavior in ultra-low frequency vibration control and ability to achieve a broad frequency bandwidth. But most relevant research on nonlinearity and active DVAs is still at the stage of theoretical study, which means that there is a long way to go from scientific research to actual structure. With this consideration, passive multiple dynamic vibration absorbers (MDVA)[12,13] are still widely used in the vibration control of structures that have multiple natural modes.

The DVA itself is a theory that should be transformed into a corresponding prototype. The cantilever DVA,[14,15] which can be equivalent to a MDVA with multi-mode vibration absorption characteristics, is commonly used in passive vibration control. Nevertheless, the high installation cost and large space requirements of the cantilever beam DVA, due to its own geometric structure limitation, makes it commonly applied in vibration control of certain large size equipment, such as an engine. As for a double cylindrical shell, a narrow space between the outside shell and inner shell makes it impossible to apply a cantilever beam DVA. For such reason, proposing a new prototype is of great importance.

The vibration characteristics of a cylinder and circular plates under different boundary conditions have been thoroughly studied.[16–19] As a combination of these simple structures, a vibration suppressor was proposed for vibration control recently. Wang et al.[20] studied the influence of low-frequency vibration suppressor material and structural parameters on the vibration acoustic radiation of a thin plate in water. However, the mechanism of vibration suppression is still not specific. Ma et al.[21] proposed a multiple band gap local resonance vibration suppressor based on the principle of dynamic vibration absorption, and verified the vibration control effect on beams through experiments and theoretical calculations. However, the plate has more complex modes, and the vibration suppressor needs to be redesigned according to these modes, and the vibration suppression effect needs to be further studied. Ma et al.[22] has also proposed a periodic vibration suppressor array with multiple secondary oscillators to suppress the low-frequency vibration, while the basic theory of this article is the band-gap theory rather than the DVA theory. Relationship between the DVA theory and the natural vibration characteristic of a suppressor needs to be studied further.

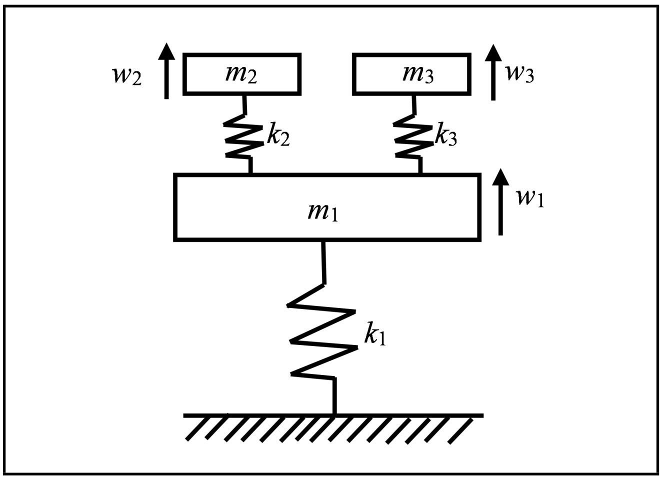

Figure 1. Parallel dynamic vibration absorber model with multiple secondary oscillators.

In this paper, we proposed a kind of multi-mode low-frequency vibration suppressor based on the principle of dynamic vibration absorption with rubber and steel as its main material. The equivalent stiffness and equivalent mass of each component is calculated theoretically. Furthermore, material parameters and geometric parameters of each component are adjusted according to the parameters of the DVA. Finally, the vibration control effect of the vibration suppressor on a four-sided simply supported plate is verified by simulation and experiment.

2. PHYSICAL MODEL

2.1. Natural Vibration Characteristics of MDVA

The DVA's multi-mode characteristics can be obtained by combining spring oscillators in series and parallel. Thus, a MDVA with parallel spring oscillators is designed to achieve this purpose, as shown in Fig. 1. The foundation of MDVA is composed of stiffness k_1 and mass m_1. The spring oscillators k_2-m_2 and k_3-m_3 are in parallel, $k = \bar{k}(1+j\gamma)$ is the complex stiffness considering the damping effect, and γ is loss factor. The structure contains three modes and is capable of meeting the multi-mode vibration suppression requirements.

In Fig. 1, w_1, w_2, w_3 is the displacement of each oscillator m_1, m_2, m_3, respectively. The natural vibration characteristics of the MDVA can be acquired by solving its natural vibration equation. The motion equation of the DVA model in Fig. 1 can be established as:

$$\begin{cases} k_1(w_1 - w) + \sum_{i=2}^{3} k_i(w_1 - w_i) + m_1\ddot{w}_1 = 0; \\ k_i(w_i - w_1) + m_i\ddot{w}_i = 0, \qquad (i = 2, 3). \end{cases} \tag{1}$$

The matrix form of Eq. (1) can be expressed as:

$$\begin{bmatrix} k_1+k_2+k_3-m_1\omega^2 & -k_2 & -k_3 \\ -k_2 & k_2-m_2\omega^2 & 0 \\ -k_3 & 0 & k_3-m_3\omega^2 \end{bmatrix} \begin{Bmatrix} w_1 \\ w_2 \\ w_3 \end{Bmatrix} = \begin{Bmatrix} 0 \\ 0 \\ 0 \end{Bmatrix}. \tag{2}$$

Equation (2) is a characteristic equation of the DVA, modal frequency of the DVA can be obtained by letting the determinant of coefficient be zero, and the determinant is essentially a cubic equation of the circular frequency ω^2, which can be expressed as:

$$a(\omega^2)^3 + b(\omega^2)^2 + c\omega^2 + d = 0; \tag{3}$$

where $a = -m_1m_2m_3$; $b = m_2m_3(k_1+k_2+k_3)+m_1m_3k_2+m_1m_2k_3$; $c = -[k_2k_3(m_1+m_2+m_3)+k_1k_3m_2+k_1k_2m_3]$; $d = k_1k_2k_3$.

Equation (3) can be used to calculate the modal frequency if parameters of MDVA are determined. This process can also be reversed, that is, to solve parameters of MDVA if modal frequency is determined. The mass of each oscillator can be determined under certain principle generally, which leaves the stiffness of the DVA to be determined. In order to achieve a better vibration suppression effect, the natural frequency of the MDVA should be consistent with that of the plate by adjusting the coefficients a, b, c, d in Eq. (3). To simplify the calculation, let $m_1 = \alpha m$, $m_2 = m_3 = m$, in which α is 3 in our study. Further analysis shows that the essence of the problem is to solve the coefficient of the cubic equation of one variable with known roots. When roots of a unary cubic equation are known, it can be expressed as:

$$A(x - x_1)(x - x_2)(x - x_3) = 0. \tag{4}$$

Equation (4) can be expanded as:

$$\begin{cases} Ax^3 + Bx^2 + Cx + D = 0; \\ B = -A(x_1 + x_2 + x_3); \\ C = A(x_1x_2 + x_2x_3 + x_1x_3); \\ D = -Ax_1x_2x_3. \end{cases} \tag{5}$$

It can be found that A, B, C, D in Eq. (5) correspond to a, b, c, d in Eq. (3), and x_1, x_2, x_3 are the known natural frequencies ω_1^2, ω_2^2, ω_3^2 of the DVA. Relationships between parameters natural frequencies can be acquired as:

$$\begin{cases} \frac{m_2m_3(k_1+k_2+k_3)+m_1m_3k_2+m_1m_2k_3}{m_1m_2m_3} = \omega_1^2 + \omega_2^2 + \omega_3^2 = P; \\ \frac{k_2k_3(m_1+m_2+m_3)+k_1k_3m_2+k_1k_2m_3}{m_1m_2m_3} = \\ \qquad \omega_1^2\omega_2^2 + \omega_2^2\omega_3^2 + \omega_1^2\omega_3^2 = Q; \\ \frac{k_1k_2k_3}{m_1m_2m_3} = \omega_1^2\omega_2^2\omega_3^2 = M. \end{cases} \tag{6}$$

Equation (6) can be further simplified by introducing α,

$$\begin{cases} \alpha mP = k_1 + (\alpha + 1)(k_2 + k_3); \\ \alpha m^2Q = k_2k_3(\alpha + 2) + k_1(k_2 + k_3); \\ \alpha m^3M = k_1k_2k_3. \end{cases} \tag{7}$$

The unary cubic equation of k_1 can be obtained from Eq. (7),

$$-k_1^3+\alpha mPk_1^2-\alpha m^2Q(\alpha+1)k_1+\alpha m^3M(\alpha+1)(\alpha+2) = 0. \tag{8}$$

The basic stiffness k_1 can be obtained by solving Eq. (8), k_2, k_3 can be obtained by substituting k_1 in Eq. (7). Generally, there are 3 roots of Eq. (8), which means 3 k_1 exist, furthermore, there should be 3 stiffness combination of the DVA. The stiffness combination should be selected according to the vibration control effect of the DVAs array and applying corresponding stiffness combination.

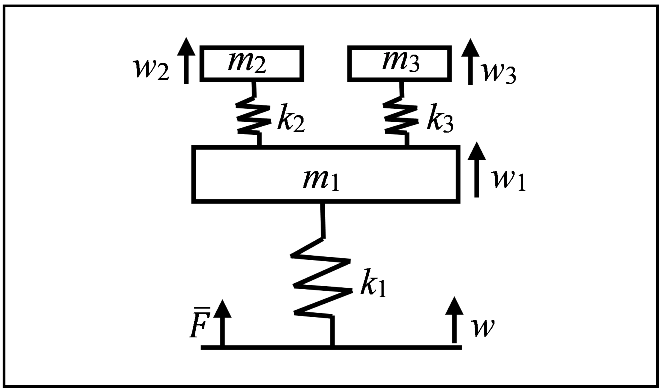

Figure 2. Schematic diagram of forced motion of multiple dynamic vibration absorber model.

2.2. Impedance Characteristics of MDVA

MDVA itself can be regarded as the additional impedance of the structure, and its impedance characteristic can also be obtained by solving Eq. (1). Although different from a natural characteristic, impedance of the DVA is related to fundamental displacement w, therefore, Eq. (1) needs to be adjusted. A schematic diagram of forced motion of MDVA is shown in Fig. 2, in which $\overline{F}$ is the exciting force.

Dynamic vibration absorber's forced equations of motion are given by:

$$\begin{cases} k_1(w_1 - w) + \sum_{j=2}^{3} k_j(w_1 - w_j) - \omega^2 m_1 w_1 = 0; \\ k_j(w_j - w_1) - \omega^2 m_j w_j = 0, \qquad (j = 2, 3); \\ k_1(w_1 - w) + \overline{F} = 0; \end{cases} \tag{9}$$

where ω is circular frequency. Define $Z = F/w$ as impedance of MDVA, where $F = -\overline{F}$ is a counteracting force. Equivalent impedance can be obtained by solving Eq. (9),

$$Z = k_1 \left[\frac{k_1}{k_1 + \sum_{j=2}^{3} \left(\frac{k_j m_j \omega^2}{\omega^2 m_j - k_j} \right) - \omega^2 m_1} - 1 \right]. \tag{10}$$

2.3. Vibration Characteristics of the Plate Attached with the DVAs Array

The forced vibration equation of a thin plate is given by:[23]

$$D\nabla^4 w(x, y, t) + \rho h \ddot{w}(x, y, t) = F_0 \delta(x - x_0)\delta(y - y_0)e^{i\omega t}; \tag{11}$$

where $\nabla^4 = \frac{\partial^4}{\partial x^4} + 2\frac{\partial^4}{\partial x^2 \partial y^2} + \frac{\partial^4}{\partial y^4}$, $D = Eh^3/(12(1-\sigma^2))$ is bending stiffness of the plate. E, ρ, h, σ are Young's module, density, thickness, and Poisson's ratio, respectively. $w(x, y, t)$ is transverse displacement and can be expanded by modal superposition,

$$w(x, y, t) = \sum_{m}^{\infty} \sum_{n}^{\infty} \phi_{mn}(x, y)\eta_{mn} e^{i\omega t}. \tag{12}$$

By substituting Eq. (12) into Eq. (11), the vibration equation can be expressed in the form of modal displacement,

$$D\nabla^4 \boldsymbol{\phi}^T \boldsymbol{\eta} - \rho h \omega^2 \boldsymbol{\phi}^T \boldsymbol{\eta} = F_0 \delta(x - x_0)\delta(y - y_0); \tag{13}$$

where $\boldsymbol{\phi}$, $\boldsymbol{\eta}$ are mode functions and the modal displacement vector, respectively. $\boldsymbol{\phi} = [\phi_{11}, \phi_{12}, \ldots, \phi_{mn}]^T$, $\boldsymbol{\eta} = [\eta_{11}, \eta_{12}, \ldots, \eta_{mn}]^T$. By multiplying both sides of Eq. (13) by $\boldsymbol{\phi}$ and integrating along the plate surface, we can get:

$$D\nabla^4 \iint_S \boldsymbol{\phi}^T \boldsymbol{\phi\eta}\, ds - \rho h \omega^2 \iint_S \boldsymbol{\phi}^T \boldsymbol{\phi\eta}\, ds = F_0 \boldsymbol{\phi}(x_0, y_0); \tag{14}$$

where mode shape function $\boldsymbol{\phi}$ satisfies following equation,

$$D\nabla^4 \phi_{mn} = \rho h \omega_{mn}^2 \phi_{mn}. \tag{15}$$

By substituting Eq. (15) into Eq. (14), the vibration equation of plate is given in matrix form,

$$(\mathbf{K} - \omega^2 \mathbf{M})\boldsymbol{\eta} = \mathbf{P}; \tag{16}$$

where $\mathbf{K} = \rho h \boldsymbol{\Omega}^2 \iint_S \boldsymbol{\phi}^T \boldsymbol{\phi\eta}\, ds$, $\mathbf{M} = \rho h \iint_S \boldsymbol{\phi}^T \boldsymbol{\phi\eta}\, ds$ are stiffness matrix and mass matrix, respectively. $\boldsymbol{\Omega}$ is a natural frequency matrix, $\mathbf{P} = F_0 \boldsymbol{\phi}(x_0, y_0)$ is a modal exciting force matrix. Modal displacement can be obtained through Eq. (16),

$$\boldsymbol{\eta} = \mathbf{P}/\rho h(\boldsymbol{\Omega}^2 - \omega^2)\boldsymbol{\phi}^T \boldsymbol{\phi}. \tag{17}$$

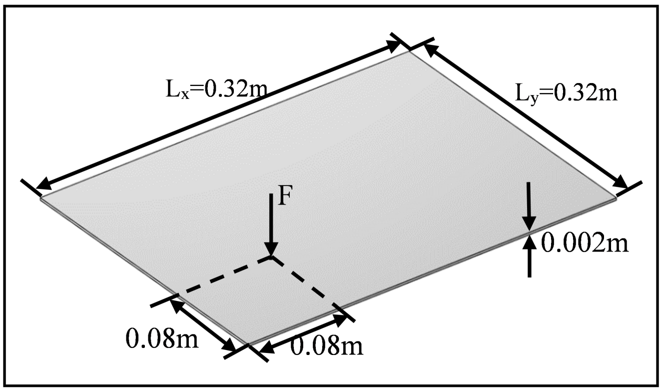

Figure 3. Model of plate under unit exciting force.

The plate's transverse displacement can be obtained by substituting Eq. (17) into Eq. (12). In this paper, a four-sided simply-supported plate is selected as a vibration control subject, whose length, width, and thickness is 0.32 m, 0.24 m, 0.002 m, respectively. The material parameters of the plate are as follows: Young's module (E) is $2e11$ Pa, density (ρ) is 7850 kg/m^3, Poisson's ratio (σ) is 0.28. A unit exciting force is applied normally to the plate at the position (0.08 m, 0.08 m), as shown in Fig. 3. In this study, average acceleration surface of the plate is used to characterize the vibration response of the plate, and in theoretical calculation, we have selected 400 points as response points (20 points in x-dimension, 20 points in y-dimension), as shown in Fig. 4. The vibration response curve is shown in Fig. 5. The selected 3 mode shapes of four-sided simply-supported plate is shown in Fig. 6.

After applying modal decoupling to the plate, vibration control design can be achieved at each mode. Accordingly,[24] the minimum equivalent mass and maximum equivalent mass appears at wave loops and wave nodes of a mode, respectively. Therefore, multi-mode vibration control of the plate can be achieved by placing the DVAs at the wave loops of each mode. As for the plate, the wave loop of the first mode is at $(\frac{l_x}{2}, \frac{l_y}{2})$, wave loops of the second mode are at $(\frac{l_x}{4}, \frac{l_y}{2})$ and $(\frac{3l_x}{4}, \frac{l_y}{2})$, and the wave loops of the fourth mode are at $(\frac{l_x}{4}, \frac{l_y}{4})$, $(\frac{3l_x}{4}, \frac{l_y}{4})$, $(\frac{l_x}{4}, \frac{3l_y}{4})$ and $(\frac{3l_x}{4}, \frac{3l_y}{4})$, and are shown as white triangles in

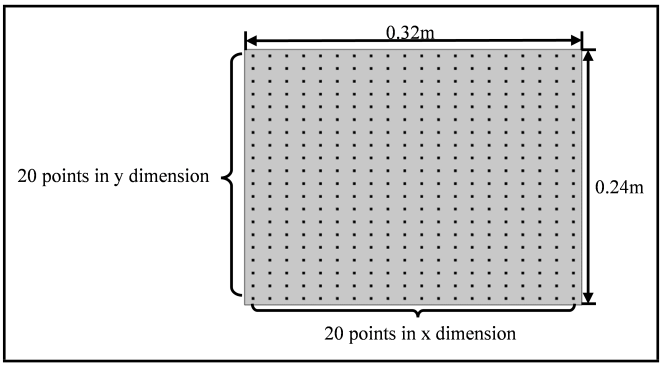

Figure 4. Response points array used in calculation of average acceleration.

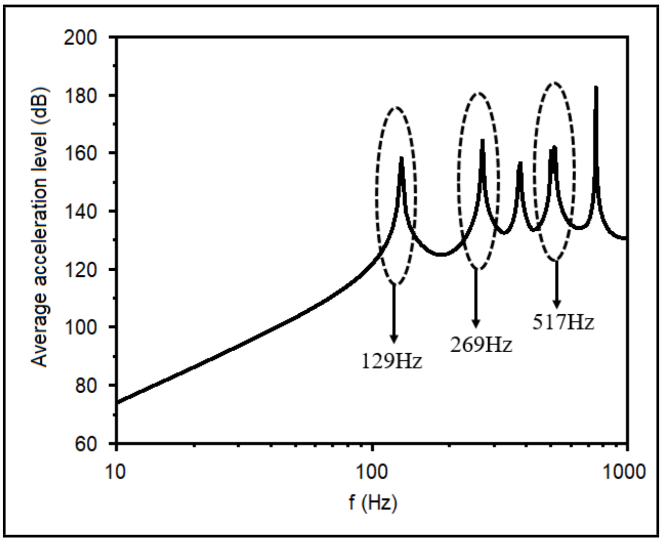

Figure 5. Vibration frequency response curve of the four-sided simply-supported plate.

Fig. 6. All of the locations combination is similar to the array, therefore, an array form is selected to simplify the location process of MDVAs, as shown in Fig. 7.

In Fig. 7, DVA1 is designed for the first mode, DVA2 is designed for the second mode, DVA3 is designed for the fourth mode. Considering that MDVA designed in Section 2 consists of 3 single DVAs and has 3 modes, therefore, the MDVAs array is arranged on the plate in Fig. 8. In the design process of the MDVA, the fundamental oscillator mass is taken as $m_1 = 0.147m_f$, secondary oscillators' masses are taken as $m_2 = m_3 = m_1/3$, in which $m_f = \rho hab$, a and b is distance between each MDVA in x-dimension and y-dimension, respectively. In this article, a is 0.108 m and b is 0.08 m.

The forced vibration equation of the plate attached with MDVAs array is given as:

$$D\nabla^4 w + \rho h\ddot{w} = F_0\delta(x - x_0)\delta(y - y_0) + \sum_{j=1}^{J} F_j\delta(x - x_j)\delta(y - y_j); \tag{18}$$

where F_j is counteracting force of each DVA applying on the plate. The motion equation of the plate attached with impedance array can be expressed as:

$$D\nabla^4 w + \rho h\ddot{w} - \sum_{j=1}^{J} Zw(x_j, y_j) = F_0\delta(x - x_0)\delta(y - y_0). \tag{19}$$

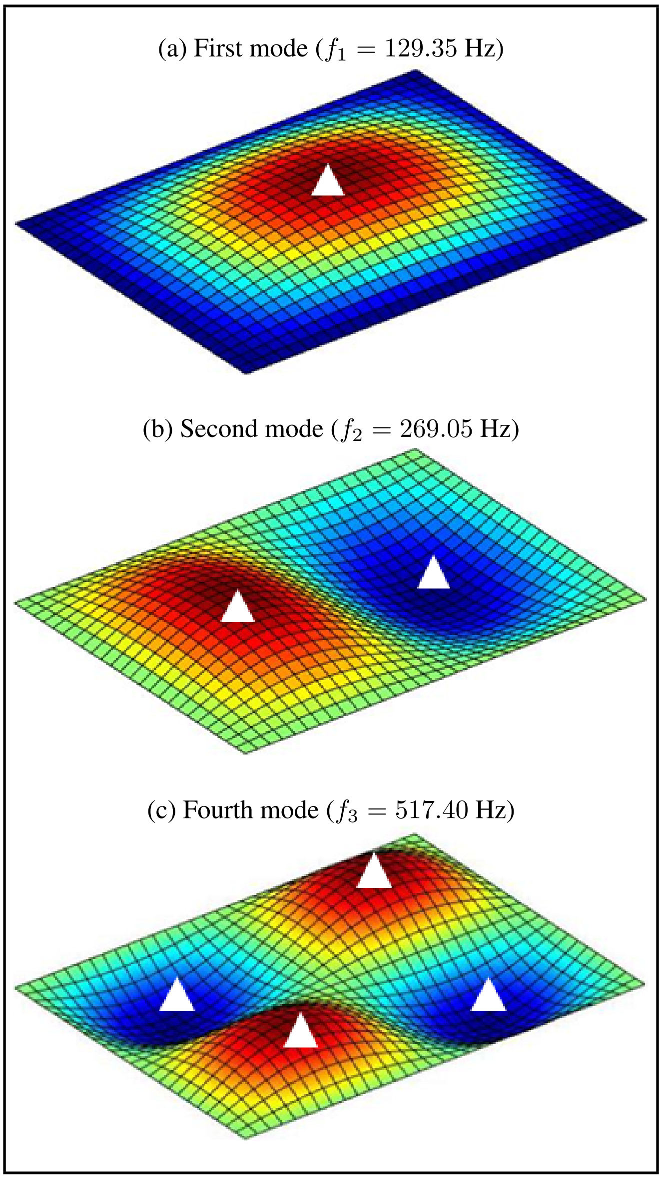

Figure 6. Modal of the four-sided simply-supported plate.

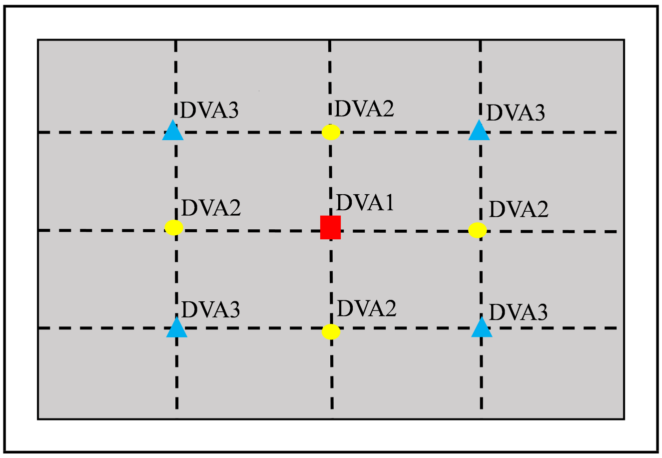

Figure 7. Distribution of single DVAs array.

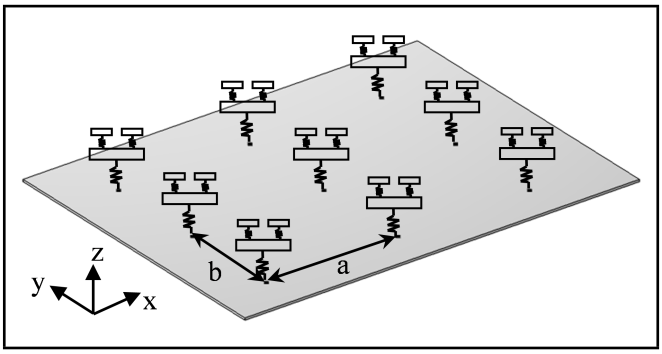

Figure 8. Model of plate attached with MDVAs array.

Table 1. Stiffness combinations solved by Eq. (8) with loss factor $\gamma = 0.1$.

	Stiffness combination 1	Stiffness combination 2	Stiffness combination 3
k1(N/m)	2.4e4*(1+0.1j)	8.28e4*(1+0.1j)	1.71e5*(1+0.1j)
k2(N/m)	4.89e4*(1+0.1j)	4.4e4*(1+0.1j)	2.22e4*(1+0.1j)
k3(N/m)	1.44e4*(1+0.1j)	4.65e3*(1+0.1j)	4.46e3*(1+0.1j)

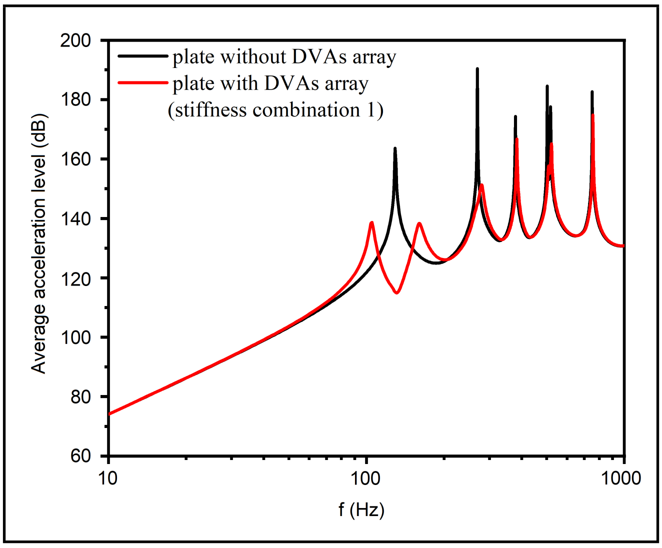

Figure 9. Vibration control effect of the DVAs array (stiffness combination 1).

Furthermore, Eq. (19) can be expressed in matrix form,

$$\left(\mathbf{K} - \omega^2\mathbf{M} - \sum_{j=1}^{J} \mathbf{Z}\boldsymbol{\phi}(x_j, y_j)^T\boldsymbol{\phi}(x_j, y_j)\right)\boldsymbol{\eta} = \mathbf{P}. \quad (20)$$

By substituting oscillator mass m_i $(i = 1, 2, 3)$ and certain frequency ω_i $(i = 1, 2, 3)$ into Eq. (8), the stiffness combinations solved are listed in Table 1.

By substituting m_i, k_i into Eq. (10), the impedance can be acquired. After substituting the impedance into Eq. (20), the vibration response curve of the four-sided simply-supported plate attached with the DVAs array can be obtained, which is shown in Fig. 9.

From Fig. 9, we can see that applying stiffness combination 1 as MDVA parameters cannot satisfy the multi-mode vibration suppression requirement, only one of the vibration absorption modes of MDVA is activated. Furthermore, we will explain this phenomenon by solving displacement transmissibility of fundamental oscillator m_1. The expression of displacement transmissibility T can be acquired by solving Eq. (10),

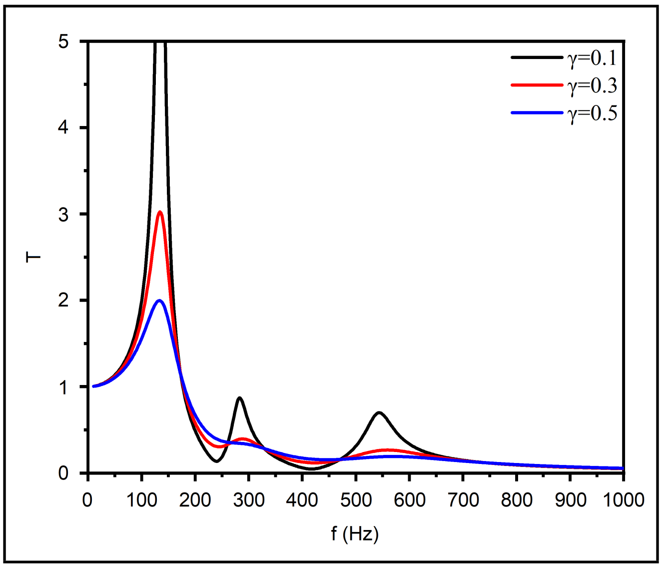

Figure 10. Displacement transmissibility frequency response curve of basic oscillator under different damping ratio (stiffness combination 1).

$$T = \frac{w_1}{w} = \frac{k_1}{k_1 - \omega^2 m_1 + \sum_{j=2}^{3}\left(\frac{k_j m_j \omega^2}{\omega^2 m_j - k_j}\right)}; \quad (21)$$

where $\omega = 2\pi f$ is natural frequency, $k_j = \overline{k}_j(1 + j\gamma)$ is the complex stiffness considering the damping effect, and γ is damping ratio. Displacement transmissibility of fundamental oscillator m_1 under different damping ratio is shown in Fig. 10.

From Fig. 10, we can see that displacement transmissibility T reaches max point when $\omega = \omega_1$, in which ω_1 is the first natural frequency of the DVA, and corresponding mode under ω_1 is longitudinal resonance mode of fundamental m_1-k_1. Thus m_1-k_1 makes up a vibration isolation system, and the vibration is difficult to be transmitted to oscillator m_2, m_3. Therefore, the DVA's second and third vibration absorption modes are not activated. Situation under the stiffness combination 2 is the same as stiffness combination 1, so it is no longer mentioned here.

Furthermore, displacement transmissibility of fundamental oscillator m_1 under different damping ratio applying stiffness combination 3 is shown in Fig. 11.

After applying stiffness combination 3 as the DVA parameters, the displacement transmissibility at three modal frequencies is greater than 1, thus vibration can be transmitted to oscillators m_2, m_3, and the second and third vibration absorption mode can be activated.

When the DVA parameters are determined, the vibration response curve of the plate attached with the DVAs array is obtained by solving Eq. (20), as shown in Fig. 12. The values of the selected three resonance peaks have been suppressed obviously when the DVAs array is applied. Therefore, the geometrical and material parameters of multi-mode low-frequency vibration suppressor will be determined according to the parameters of the MDVA under the stiffness combination 3.

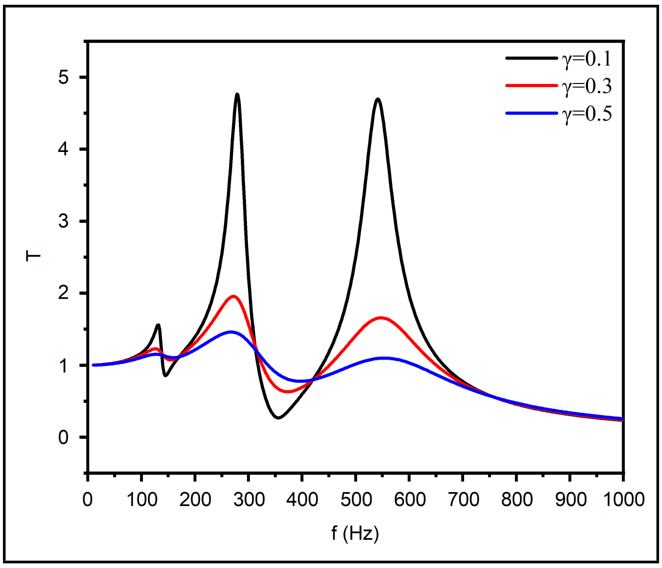

Figure 11. Displacement transmissibility frequency response curve of basic oscillator under different damping ratio (stiffness combination 3).

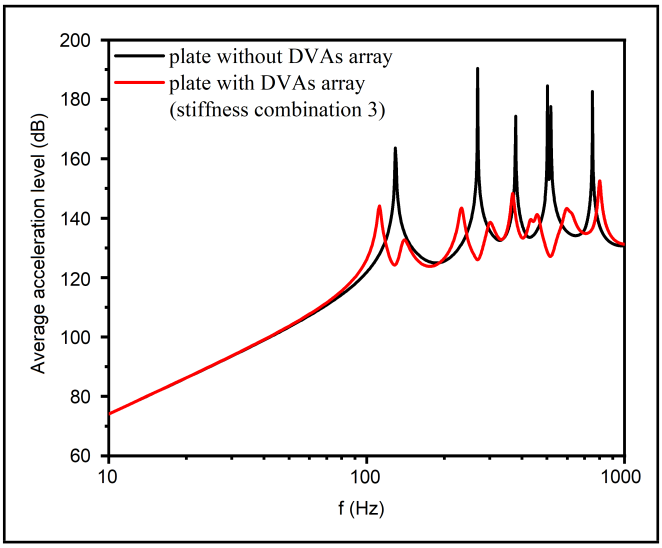

Figure 12. Vibration control effect of the DVA array (stiffness combination 3).

3. DESIGN OF MULTI-MODE LOW-FREQUENCY VIBRATION SUPPRESSOR

The preliminary model of the suppressor is shown in Fig. 13. The main component is: a rubber basis, a metal skeleton, two rubber plates, and two mass blocks. The rubber basis and rubber plate are used to provide stiffness and damping, corresponding to k_1, k_2, k_3, the metal skeleton and mass block are used to provide mass, corresponding to m_1, m_2, m_3.

3.1. Structure Design of Rubber Plate Attached with Mass Block

The natural vibration fundamental equation of round plate is given as:[23]

$$D\nabla^4 w + \rho h \frac{\partial^2 w}{\partial t^2} = 0; \tag{22}$$

where D, ρ is bending stiffness and density of the plate, respectively. $\nabla^2 = \frac{1}{r}\frac{\partial}{\partial r}\left(r\frac{\partial}{\partial r}\right) + \frac{1}{r}\frac{\partial^2}{\partial \theta^2}$ is Laplace operator in polar coordinate. Assuming the solution of Eq. (22) as:

$$w(r,\theta,t) = W(r,\theta)e^{i\omega t}; \tag{23}$$

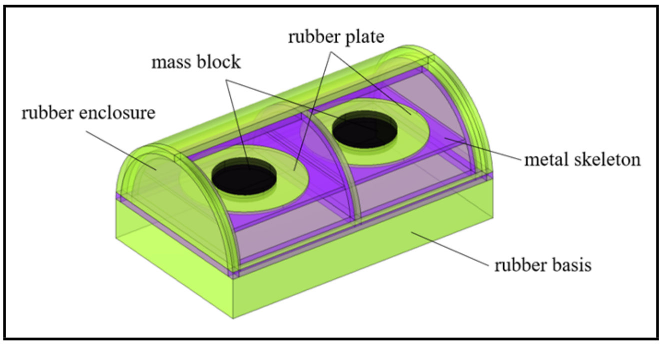

Figure 13. Preliminary design model of multiple-mode low-frequency vibration suppressor.

the vibration mode equation can be acquired by substituting Eq. (23) into Eq. (22),

$$(\nabla^4 - k^4)W = 0; \tag{24}$$

in which $k^4 = \omega^2\frac{\rho h}{D}$ is the natural frequency coefficient. By applying the variable separation method, the general solution of Eq. (24) can be acquired as:

$$W(r,\theta) = \sum_{m=1}^{\infty}\Big[A_m J_m(kr) + B_m I_m(kr) + C_m Y_m(kr) + D_m K_m(kr)\Big]\cos m\theta. \tag{25}$$

A round plate centrally attached with a mass block is considered when its boundary is clamped. The boundary condition can be expressed in following form:[18,23]

$$\begin{cases} W(a,\theta) = 0; \\ \frac{\partial W(a,\theta)}{\partial r} = 0; \\ \frac{\partial W(b,\theta)}{\partial r} = 0; \\ 2\pi b V_r + m_b\omega^2 W(b,\theta) = 0; \end{cases} \tag{26}$$

where a is radius of the plate, b, h_0, ρ_0, m_b is radius, height, density, and mass of mass block, respectively. V_r is Kirchhoff shearing stress. Linear equations of A_m, B_m, C_m, D_m can be acquired by substituting Eq. (25) into Eq. (26). The fundamental frequency coefficient μ_0 can be acquired by letting the coefficient determinant be equal to zero and letting $m = 0$, and fundamental frequency corresponding to axial mode can be obtained as:

$$f_0 = \frac{\mu_0^2}{2\pi a^2}\sqrt{\frac{D}{\rho}}. \tag{27}$$

The fundamental frequency can also be expressed in the form of equivalent stiffness k_{eq} and equivalent mass m_{eq},

$$f_0 = \frac{1}{2\pi}\sqrt{\frac{k_{eq}}{m_{eq}}}. \tag{28}$$

.

Young's module of plate is acquired by associating Eq. (27) and Eq. (28),

$$E = \frac{12k_{eq}a^4(1-\sigma^2)\rho}{\mu_0^4 h^2 m_{eq}}; \tag{29}$$

in which k_{eq} and m_{eq} is equivalent stiffness and equivalent mass of annular plate attached with mass block under first

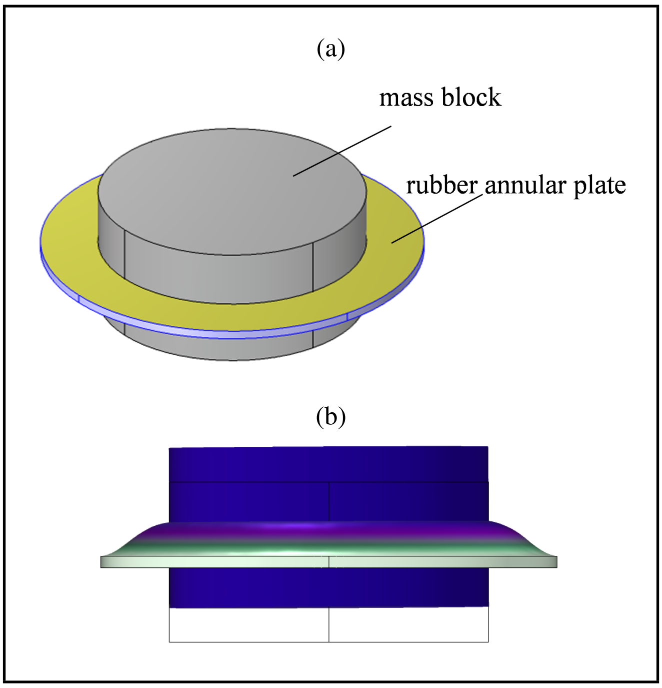

Figure 14. (a) Annular plate clamped on outside with rigid mass inside. (b) Axial mode of annular plate clamped on outside with rigid mass on inside calculated by FEM method ($f_0 = 292.5$ Hz).

mode (axial resonance mode), respectively. σ is Poisson's ratio of the plate.

By substituting m_2 and k_2 into Eq. (28), fundamental frequency f_0 can be calculated analytically, and the value is 292.63 Hz. The error between theoretical solution and FEM solution is only 0.04%, which verified the correctness of the equivalent progress.

3.2. Structure Design of Rubber Basis Attached with Metal Skeleton

The rubber basis of preliminary vibration suppressor is a cuboid elastomer, whose equivalent stiffness can be expressed as:[17]

$$k = \frac{ESm_n}{h}; \tag{30}$$

where E, S, h is cuboid elastomer's Young's module, area of cross section, height, respectively. $m_n = (1 \sim 1.5)n^2$ is shape coefficient, where $n = S_l/S_f$, S_l and S_f is constraint area and free area of cuboid elastomer.[17] When cuboid elastomer is attached with a mass block of the same cross section area, the axial resonance modal frequency of combination is:

$$f_0 = \frac{1}{2\pi}\sqrt{\frac{k_{eq}}{m_{eq}}}. \tag{31}$$

The mass of the elastomer cannot be ignored in the equivalent process. So the equivalent mass $m_{eq} = m_1 + m_2/3$, where m_1 is the mass of the attached mass block, m_2 is the mass of the cuboid elastomer.[17] In Eq. (31), k_{eq} is the equivalent stiffness. From Eq. (30), Young's module of fundamental rubber can be obtained as:

$$E = \frac{k_{eq}h}{Sm_n}. \tag{32}$$

By substituting m_1 and k_1 into Eq. (31), the fundamental frequency f_0 can be calculated analytically, and the value is

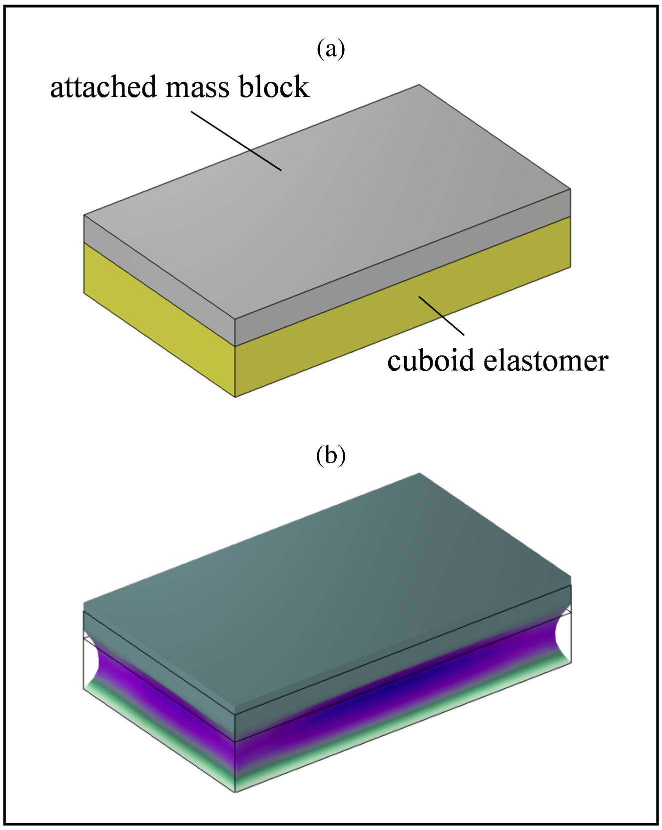

Figure 15. (a) Model of the cuboid elastomer attached with additional mass. (b) Axial mode of cuboid elastomer attached with additional mass calculated by FEM method ($f_0 = 467.25$ Hz).

467.53 Hz. The error between the theoretical solution and the FEM solution is only 0.06%.

Furthermore, by setting the mass of the metal skeleton the same as that of the attached mass shown in Fig. 15(a), the same axial mode can be obtained. Considering the preliminary model of the suppressor, the final version of the vibration suppressor is shown in Fig. 16(a). The purpose of the holes on the metal skeleton is to decrease weight. The result shows that the axial mode frequency of the cuboid elastomer attached with the metal skeleton and the rubber enclosure is nearly the same as cuboid elastomer attached with the mass block in the same mass, and the error is 0.67, which verified the correctness of the equivalent process.

3.3. Vibration Control Effect of Suppressors Array

According to the equivalent theory mentioned in Section 3.2, the geometric and material parameters of each component of the suppressor are determined. The final design model of a horizontal multi-mode low frequency suppressor is shown in Fig. 17. The model of the four-sided simply-supported plate attached with vibration suppressors array is shown in Fig. 18. The material parameters of the components of vibration suppressor is shown in Table 2.

We have selected COMSOL as the simulation software to verify the vibration control effect of suppressors array designed in Section 3.1–3.2. The three selections are needed in pre-setup procedure, which is space dimension selection, physics interface selection, and the study selection. In FEM, the four-sided simply-supported boundary condition is

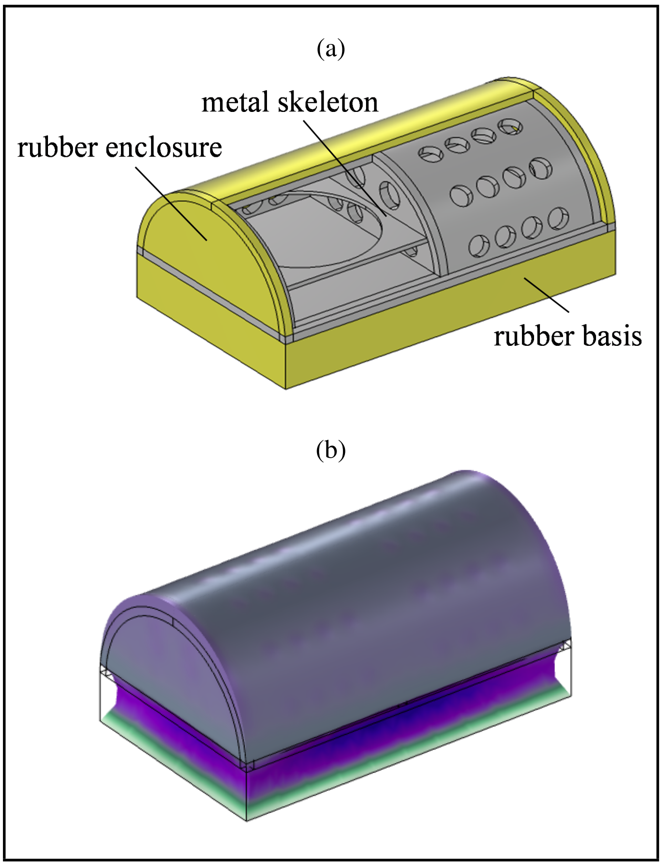

Figure 16. (a) Model of the cuboid elastomer attached with the metal skeleton and the rubber enclosure. (b) Axial mode of the cuboid elastomer attached with the metal skeleton and the rubber enclosure calculated by FEM method ($f_0 = 464.38$ Hz).

Table 2. Material parameters of components of vibration suppressor.

	Young's module E (Pa)	Poisson's ratio σ	Density ρ (kg/m^3)	Damping ratio γ
Mass block	2e11	0.28	7850	0.001
Metal skeleton	7e10	0.35	2700	0.001
Rubber basis	2.73e5	0.49	1100	0.1
Rubber plate(left)	1.75e6	0.49	1100	0.1
Rubber plate(right)	4.11e6	0.49	1100	0.1

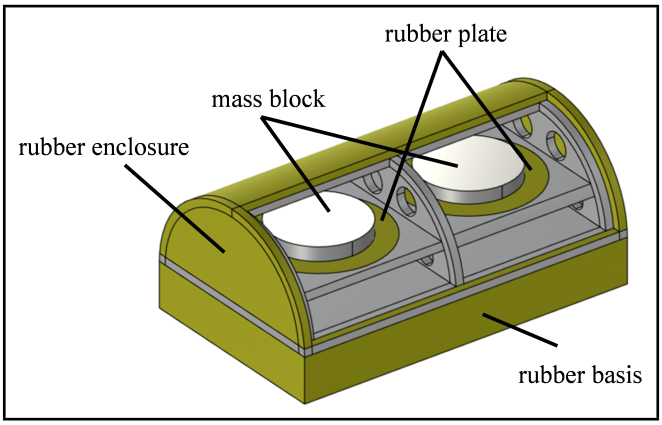

Figure 17. Final design model of horizontal multi-mode low frequency suppressor.

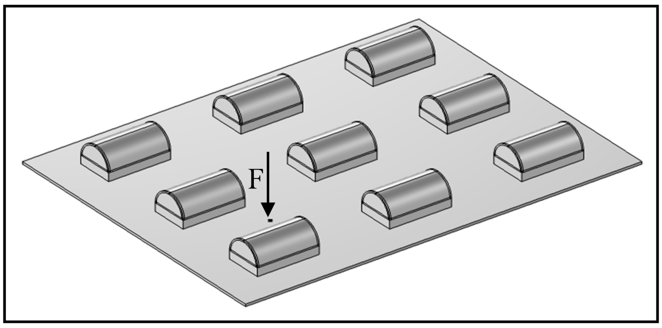

Figure 18. Four-sided simply-supported plate attached with vibration suppressors array.

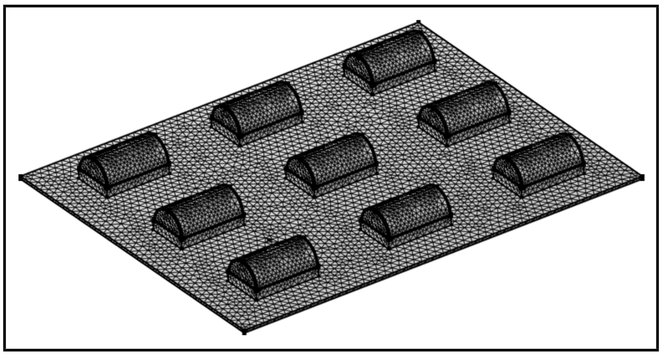

Figure 19. Schematic diagram of mesh.

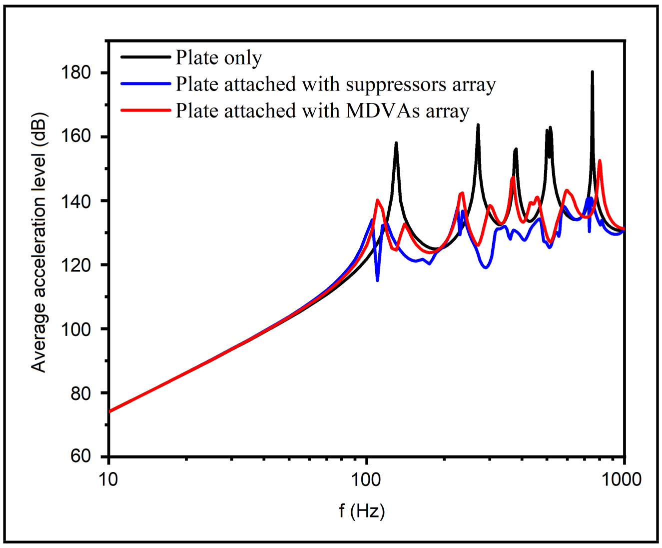

Figure 20. Control effect of the DVAs array and suppressors array.

achieved by prescribing displacement of each sides of the plate, which is, by limiting their tangential displacement. As a result, the normal displacement is free. The schematic diagram of mesh is shown in Fig. 19. The control effect of the DVAs array and suppressors array is shown in Fig. 20.

From Fig. 20, the result shows that the vibration control effect of plate attached with the DVAs array and suppressors array is obviously, and the resonance peak of the vibration response curve is eliminated in both situations. After applying the suppressors array, the average acceleration level of the plate within the calculated frequency range has decreased by an average of 5.57 dB. At the first resonance peak ($f = 130$ Hz), the average acceleration level of the plate has decreased by 31.77 dB. At the second resonance peak ($f = 270$ Hz), the av-

(a) Plate under four-sided simply-supported boundary condition

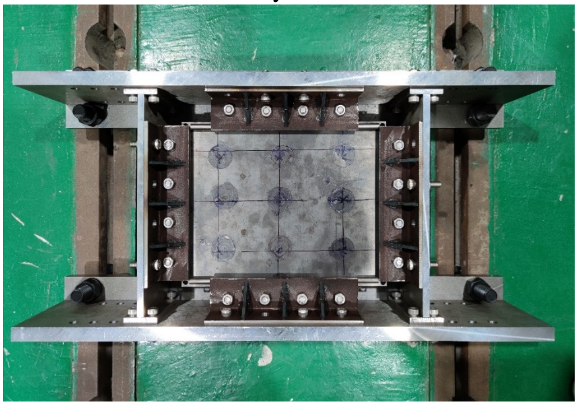

(b) Plate attached with suppressors array

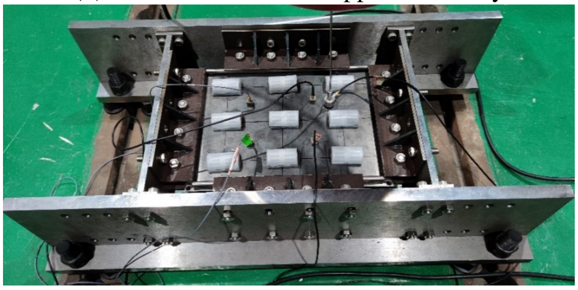

Figure 21. Photographs of experiment site.

erage acceleration level of the plate has decreased by 31.77 dB. At the third resonance peak ($f = 515$ Hz), the average acceleration level of the plate has decreased by 37.44 dB. The contact form between the suppressors array and the plate is surface contact, which is different from the point contact between the DVAs array and the plate, therefore damping plays a more important role when applying the suppressors array.

4. EXPERIMENT VERIFICATION

A multi-mode vibration suppressor is designed in Section 3, and the simulation result shows that the vibration response of the resonance peak of the plate is significantly suppressed after applying with the suppressors array. But the correctness of the simulation result still needs to be verified by the experiment. Therefore, it's necessary to carry out the experiment verification.

To simulate the four-sided simply-supported boundary condition as much as possible, fixtures were designed and manufactured specially for the purpose of fastening the plate. The schematic diagram of the experiment model is shown in Fig. 21. The experiment equipment is shown in Fig. 22.

In experiment, the signal from the signal source is driven by the power amplifier, and the exciter is connected with the plate through a force sensor to collect the excitation force. The admission data of each measuring point can be obtained after the signal collected by the acceleration sensor is normalized by the excitation point force signal. The schematic diagram of the experiment system is shown in Fig. 23.

The main vibration suppression performance index of this experiment is the mechanical admittance, which is defined as

(a) UTG9010C signal source

(b) MB500VI power amplifier

(c) MB Dynamics exciter

(d) INV3062V data acquisition analyzer

Figure 22. Photographs of experiment equipments.

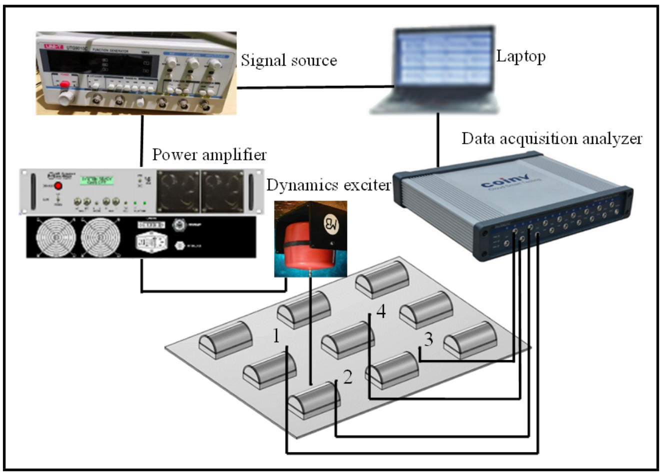

Figure 23. Schematic diagram of the experiment system.

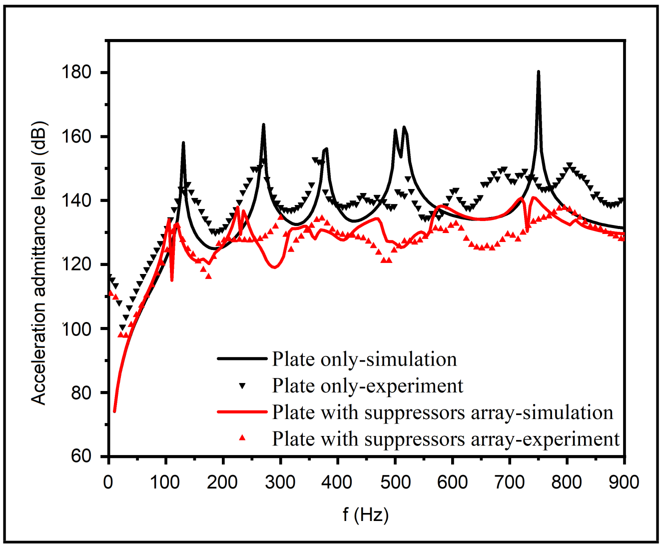

Figure 24. Comparison curve of the vibration control effect of the suppressors array.

the reciprocal of the mechanical impedance, namely the vibration response under unit steady-state force excitation. Usually, it is impossible to ensure the excitation is always the unit excitation in the experiment. Therefore, the concept of the mechanical admittance is introduced to normalize the vibration response, which is helpful to compare and analyze the simulation results. According to the position of test point, mechanical admittance can be divided into input admittance and transfer admittance. Input admittance is defined as the ratio of the vibration response to the excitation force amplitude at the position of excitation point. Transfer admittance is defined as the ratio of the vibration response to the excitation force amplitude at the position of the non-excitation point. The mechanical admittance in this experiment is the acceleration transfer admittance, whose expression is:

$$Y = \frac{a}{F}. \tag{33}$$

The average acceleration admittance level is obtained by:

$$L = 10\log\left(\frac{1}{n}\sum_{i=1}^{n}(Y_i)^2\right) + 120; \tag{34}$$

where i is the serial number of the measure point. The comparison of the experiment results and simulation results is shown in Fig. 24.

It can be shown from Fig. 24 that simulation and experimental results are basically consistent. And compared with the simulation results, the experimental results show lower vibration response in most frequency bands, which is because the structural damping in the simulation is not exactly the same as that in the actual structure, as well as bonding between the actual structure and the plate will further increase the influence of damping on the vibration control. After attachment with the suppressors array, the peak response of the plate at the selected resonant frequency decreases significantly, and the vibration response in the test frequency band decreases by 9.63 dB on average, which can verify the vibration control effect of the suppression array on the plate.

5. CONCLUSIONS

Firstly, the vibration characteristic of the simply supported plate was studied, and the vibration control strategy was determined to suppress the low frequency resonance peak of the plate through the MDVAs array. The low frequency resonance peak of the plate was suppressed by selecting the parameters of the DVA reasonably. Then a low-frequency vibration suppressor with multi-mode characteristics was proposed, whose equivalent stiffness and equivalent mass of each part was theoretically calculated. The material parameters and the geometric parameters of each component were adjusted based on parameters of the MDVA. Finally, the vibration control effect of the multi-mode low frequency suppressors array was verified through simulation and experiment. The analysis leads to the following conclusions:

1. Both the MDVAs array and the vibration suppressors array designed based on the parameters of the MDVA have certain control effects on the selected resonance peak, and vibration suppressors array had a better performance. The reason was that the contact form between the plate and the vibration suppressors array was surface contact, which makes the effect of damping in the vibration control more significant;

2. In order to realize the multi-mode vibration control, the axial resonance frequency of the rubber basis attached with the metal skeleton must be corresponding to the highest frequency of the selected resonance peak, in case of vibration isolation. Otherwise, the vibration cannot be transmitted to the rest component of suppressor; and,

3. Although the designed suppressors array's vibration control effect to the resonance peak of vibration response curve of the plate is obvious, there are two resonance peaks on both sides of the original peaks, especially the first peak. So, there was great space for further optimization.

ACKNOWLEDGEMENTS

This work was supported by Jiangsu Natural Science Youth Foundation (BK20200995) and the Foundation Strengthening Program Technical Area Fund (2020-JCJQ-JJ-228).

REFERENCES

1 Cheng, Y., Li, D., and Li, C. Dynamic vibration absorbers for vibration control within a frequency band, *Journal of Sound and Vibration*, **330** (8),1582–1598, (2011). https://doi.org/10.1016/j.jsv.2010.10.018

2 Jacquot, R. G. Suppression of random vibration in plates using vibration absorbers, *Journal of Sound and Vibration*, **248** (4), 585–596, (2001). https://doi.org/10.1006/jsvi.2001.3558

3 Estéve, S. J. and Johnson, M. E. Reduction of sound transmission into a circular cylindrical shell using distributed vibration absorbers and Helmholtz resonators, *The Journal of the Acoustical Society of America*, **112** (6), 2840–2848, (2002). https://doi.org/10.1121/1.1514933

4 Huo, G., Chen, Z., Jiao, Y., and Zhu, X. Optimization of dynamic vibration absorbers for suppressing sound radiation of plate structures, *Journal of Vibration and Acoustics*, **143** (2), (2021). https://doi.org/10.1115/1.4048168

5 Frahm, H. Device for damping vibrations of bodies: US, US989958 A., (1911).

6 Chang, Y., Zhou, J., Wang, K., and Xu, D. A quasi-zero-stiffness dynamic vibration absorber, *Journal of Sound and Vibration*, **494**, 115859, (2021). https://doi.org/10.1016/j.jsv.2020.115859

7 Lin, S., Zhang, Y., Liang, Y., Liu, Y., Liu, C., and Yang, Z. Bandgap characteristics and wave attenuation of metamaterials based on negative-stiffness dynamic vibration absorbers, *Journal of Sound and Vibration*, **502**, 116088, (2021). https://doi.org/10.1016/j.jsv.2021.116088

8 Wang, X., He, T., Shen, Y., Shan, Y., and Liu, X. Parameters optimization and performance evaluation for the novel inerter-based dynamic vibration absorbers with negative stiffness, *Journal of Sound and Vibration*, **463** (3), 114941, (2019). https://doi.org/10.1016/j.jsv.2019.114941

9 Beltrán-Carbajal, F. and Silva-Navarro, G. Active vibration control in Duffing mechanical systems using dynamic vibration absorbers, *Journal of Sound and Vibration*, **333** (14), 3019–3030, (2014). https://doi.org/10.1016/j.jsv.2014.03.002

10 Kassem, M., Yang, Z., Gu, Y., Wang, W., and Safwat, E. Active dynamic vibration absorber for flutter suppression, *Journal of Sound and Vibration*, **469**, 115110, (2020). https://doi.org/10.1016/j.jsv.2019.115110

11 Rasid, S., Mizuno, T., Ishino, Y., Takasaki, M., Hara, M., and Yamaguchi, D. Design and control of active vibration isolation system with an active dynamic vibration absorber operating as accelerometer, *Journal of Sound and Vibration*, **438**, 175–190, (2018). https://doi.org/10.1016/j.jsv.2018.09.037

12 Li, H., Wu, S., Chen, Q., and Fei, Q. Design of dynamic absorbers to control the flexural resonant vibration of structures characterized by multiple natural modes, *Journal of Sound and Vibration*, **513**, 116415, (2021). https://doi.org/10.1016/j.jsv.2021.116415

13 Noori, B., Arcos, R., Clot, A., and Romeu, J. Control of ground-borne underground railway-induced vibration from double-deck tunnel infrastructures by means of dynamic vibration absorbers, *Journal of Sound and Vibration*, **461**, 114914, (2019). https://doi.org/10.1016/j.jsv.2019.114914

14 Lim, S., Kim, K., Cho, U., Park, N.-C., Park, Y.-P., Park, K.-S., and Soh, W.-Y. Cantilever dynamic vibration absorber for reducing optical disk drive vibration, *IEEE Transactions on Magnetics*, **45** (5), 2198–2201, (2009). https://doi.org/10.1109/tmag.2009.2016144

15 Li, H., Lou, J., Zhu, S., et al. Modeling and vibration absorption performance analysis of cantilever beam-type dynamic vibration absorber, *Journal of Wuhan University of Technology (Transportation Science & Engineering)* (in Chinese), 171–174, (2013).

16 Leissa, A. W. *Vibration of Plates*, Scientific and Technical Information Division, National Aeronautics and Space Administration, (1969).

17 Lin, K. *Rubber Industry Handbook, The sixth volume: Industrial rubber product* (in Chinese), Chemical Industry Press, (1993).

18 Wang, C. Y. Vibration of a circular plate with an attached core, *Journal of Sound and Vibration*, **280** (3–5), 1075–1082, (2005). https://doi.org/10.1016/j.jsv.2004.02.029

19 Weisensel, G. N. Natural frequency information for circular and annular plates, *Journal of Sound and Vibration*, **133** (1), 129–137, (1989). https://doi.org/10.1016/0022-460x(89)90987-5

20 Wang, Y., Tao, M., and Fu, L. Low-frequency vibration suppressor applied in suppressing vibration and acoustic radiation of underwater thin plate, *Journal of Vibration and Shock* (in Chinese), **39** (21), 233–240, (2020). https://doi.org/10.13465/j.cnki.jvs.2020.21.031

21 Ma, J., Sheng, M., and Han, Y. Design and experimental verification of multiple band gap local resonance unit, *Journal of Vibration Engineering* (in Chinese), **32** (06), 943–949, (2019). https://doi.org/10.16385/j.cnki.issn.1004-4523.2019.06.002

22 Ma, J., Sheng, M., Guo, Z., and Qin, Q. Dynamic analysis of periodic vibration suppressors with multiple secondary oscillators, *Journal of Sound and Vibration*, **424**, 94–111, (2018). https://doi.org/10.1016/j.jsv.2018.03.002

23 Cao, Z. *Vibration Theory of Plate and Shell* (in Chinese), China Railway Publishing House Co., (1989).

24 Seto, K. *Dynamic Vibration Absorber and Its Applications* (in Chinese), China Machine Press, (2013).